Journal of Hydrology 567 (2018) 579–589

Contents lists available at ScienceDirect

Journal of Hydrology

journal homepage: www.elsevier.com/locate/jhydrol

Research papers

Penalized maximum likelihood estimators for the nonstationary Pearson type 3 distribution

Song Xinyi[a], Lu Fan[a,*], Wang Hao[a], Xiao Weihua[a], Zhu Kui[b]

[a] State Key Laboratory of Simulation and Regulation of Water Cycle in River Basin, China Institute of Water Resources and Hydropower Research, Beijing 100038, China
[b] School of Resources and Earth Science, China University of Mining and Technology, Xuzhou 221116, China

ARTICLE INFO

This manuscript was handled by Andras Bardossy, Editor-in-Chief, with the assistance of Anne-Catherine Favre, Associate Editor

Keywords:
Pearson type 3 distribution
Nonstationary condition
Parameter estimation
Penalized maximum likelihood estimation

ABSTRACT

The climate change and human activities can principally doubt the frequency analysis methods which assume that the hydrological events are stationary. The Pearson type 3 (P3) distribution, which has been widely applied in frequency analysis under the stationary condition, was developed for the nonstationary cases. The distribution parameters can be expressed as exponential or polynomial functions with time or other covariates. Parameter estimation for the nonstationary P3 model was done with the penalized maximum likelihood estimation (PMLE) method in which we applied a restrictive penalty on the location parameter to avoid unreasonable results. The results of the nonstationary P3 model were compared to that of the generalized extreme value (GEV) distribution, in which the generalized maximum likelihood estimation (GMLE) method was applied to estimate the parameters. The Monte Carlo simulations indicated that the nonstationary P3 model provided better results than the nonstationary GEV model for different sample sizes. Both models were also applied in hydrological series with various trends and record lengths to prove the feasibility of the nonstationary P3 model in practical applications. The applications showed that the nonstationary P3 model performed better than the nonstationary GEV model in most of the studied cases.

1. Introduction

To meet the demand of project design, the extreme value theory provides a method to explain historical records and to make inference for future probabilities of extreme events (i.e., floods, wind speeds, extreme waves, and rainfall). The log Pearson type 3 (LP3) distribution was commonly recommended to fit sequences of annual peak flood flows in the United States (Benson, 1968). Moreover, the Pearson type 3 (P3) distribution was recommended for frequency analysis by the Ministry of Water Resources of the People's Republic of China (Zhan and Ye, 1987). Since then, the P3, LP3 and gamma family of distributions were considered in a large number of related studies, such as precipitation, annual runoff and flood series (Durrans, 1992). To analyze the eco-hydrological conditions in the Yellow River, Zhang et al. (2013) used the stationary P3 distribution to conduct the frequency analysis for stream flow. For the low flow frequency analysis, Yu et al. (2014) found that the stationary P3 distribution is usually able to give the most satisfactory results when compared to that of Weibull and copula-based distributions. Except for frequency analysis, Zucco et al. (2015) used the P3 distribution to fit runoff series, wherein the parameters in the distribution were peak discharge, time to peak and shape parameter, respectively. However, there is by no means universal acceptance of the P3 distribution for modeling hydrological events. The advances in both at-site and regional frequency analyses caused debates, which were related to the utilization of P3 distribution, among statistical hydrologists (Vogel and McMartin, 1991). For example, Ribeiro-Correa and Rousselle (1993) developed an estimation methodology for a regional P3 flood flow model. However, Hosking and Wallis (1993) suggested to use the generalized extreme value (GEV) distribution because the sample L skewness and L kurtosis were unbiased, and the generalized logistic distribution was recommended as the standard for regional flood frequency analysis in the UK (Kjeldsen and Jones, 2006).

During the past decades, numerous methods have been developed to estimate the P3 distribution parameters and to conduct frequency analysis (Bobée, 1973; Singh and Singh, 1985; Song and Ding, 1988; Durrans, 1992). Cohen (1950) introduced the method of moments, which was later recommended by the US Water Resources Council (Durrans, 1992). Harter (1969) provided a detailed table of percentage points for the P3 distribution. Matalas and Wallis (1973) found that the maximum likelihood estimation (MLE) method yielded solutions that were less biased and less variable when compared to the moment

* Corresponding author.
E-mail address: lufan@iwhr.com (F. Lu).

https://doi.org/10.1016/j.jhydrol.2018.10.035
Received 22 July 2018; Received in revised form 15 October 2018; Accepted 17 October 2018
Available online 18 October 2018

estimates. Similar conclusions were confirmed by other researchers (Buckett and Oliver, 1977; Song and Ding, 1988; Ding et al., 1989). On the contrary, Nozdryn-Plotnicki and Watt (1979) used MLE, the method of moments and a method which preserved the moments of untransformed flows to estimate the parameters, and they argued that no one method be superior for the whole of the parameter space. Singh and Singh (1985) also pointed that the method of moments with a corrected coefficient of skewness C_s provided better results than the MLE method. However, the traditional frequency analysis was based on two fundamental assumptions: the data series should be independent and identically distributed. Previous studies indicated that extreme events were hardly stationary due to the influence of climate change and human activity, and significant trends can be detected in extreme values from different hydro-climatological series (Milly et al., 2008; IPCC, 2014). Lin et al. (2014) pointed out that the land use change was more likely to affect runoff during the flood season. In further, the social economy was significantly affected by the extreme climatic factors (He et al., 2017). As a result, the nonstationary model with time-varying parameters was progressively popular in recent two decades, which challenged the uses of the method of moments that may only be valid for the stationary conditions.

Although the P3 distribution is still considered as an alternative in regional frequency analysis (Yang et al., 2010; San et al., 2011), it has no longer be applied in the hydrology to the same extent as others under the nonstationary condition. For example, the nonstationary GEV model is prevalent in recent hydrologic literature, and has been extensively used for flood frequency analysis (Coles, 2001; Adlouni et al., 2007; Cannon 2010; Lima et al., 2015). The GAMLSS package also has widely been used in hydrological frequency analysis in recent years (López and Francés, 2013; Li and Tan, 2015). The GAMLSS package in R project provides a number of continuous, discrete and mixed distributions for modelling the data series, but it only includes a two-parameter Gamma distribution (Stasinopoulos et al., 2008). Therefore, this paper aimed to develop a method for the nonstationary P3 distribution. Besides, we can conduct further works based on the fitted P3 distribution. For example, it is able to compare the performance of different parameter estimation methods, and analyze the reliability of results based on uncertainty estimation. In recent years, some studies also reported that the P3 distribution could generate the most satisfactory results in at-site and regional analysis (Saf, 2009; Dodangeh et al., 2014; Yu et al., 2014). To our knowledge, the P3 distribution was hardly used to fit the nonstationary time series. Liu et al. (2014) studied the performance of different distributions under the nonstationary conditions and pointed that the GEV and P3 models can better fit sample than other models. However, unlike the usual method which adopted the time-varying parameters in a nonstationary model, Liu et al. (2014) used the nonstationary modeling by modifying the nonstationary series to stationary series.

The objective of this study is to use the P3 distribution for estimating design values under the nonstationary conditions. A penalized maximum likelihood estimation (PMLE) method is used for parameter estimation in the case of a nonstationary P3 model. This method avoids unreasonable results in the nonstationary condition by setting a penalized term to restrict the value of the location parameter. The parameters are expressed as a polynomial function of time t to show the feasibility of PMLE. If the nonstationary P3 distribution performs well in this case, we believed that it can generate satisfied results when using other covariates. The parameters can also be dependent on other covariates, i.e., climate indices. Before selecting other covariates, it is better to quantitatively understand the effects of climate and human factors on the hydrological process. Thus, we do not consider other covariates in this paper. The results of nonstationary P3 models are compared to that of nonstationary GEV models, which is the most popular model for annual maximum/minimum series. The nonstationary GEV parameters are estimated by the generalized maximum likelihood estimation (GMLE) method, which can avoid the problem in numerical technique when employing the MLE method in small samples (Martins and Stedinger, 2000; Adlouni et al., 2007). Moreover, we use the extRemes package in R project to build the nonstationary GEV model. The performance of both models is verified by Monte Carlo simulation and case studies.

2. Methods

2.1. Nonstationary Pearson type 3 model

2.1.1. Model structure

The Pearson type 3 distribution is bounded in one direction according to the shape parameter, and its probability density function is as follows:

$$f(x) = \frac{\beta^{\alpha}}{\Gamma(\alpha)}(x-r)^{\alpha-1}\exp[-\beta(x-r)] \tag{1}$$

where α, β, r are the shape, scale and location parameters, respectively. In general, the P3 distribution has five forms according to the shape parameter α, and previous research indicated that it would be more suitable when $\alpha > 2$ (Buckett and Oliver, 1977). If the scale parameter $\beta > 0$, the P3 distribution has a positive skewness and $x - r \geqslant 0$, while the distribution has a negative skewness and $x - r \leqslant 0$ when $\beta < 0$ (Koutrouvelis and Canavos, 1999). As we are interested in the frequency of extreme value with a high quantile, the shape and scale parameters are supposed to be positive values in this paper.

In the stationary case, the traditional parameter estimation method is used the first four moments of the population to obtain the three parameters of the P3 distribution. According to the sample series, these parameters can be expressed as the equations from the mean value $\bar{x}$, coefficient of variation C_v and coefficient of skewness C_s (Zhang et al., 2013):

$$\begin{cases} \alpha = \frac{4}{C_s^2} \\ \beta = \frac{2}{\bar{x}C_vC_s} \\ r = \bar{x}\left(1 - \frac{2C_v}{C_s}\right) \end{cases} \tag{2}$$

However, the method is no longer be valid under the nonstationary assumption. Therefore, the maximum likelihood estimation (MLE) method is used in this paper to obtain the time-varying parameters of the nonstationary P3 distribution. The parameters in a nonstationary P3 distribution model will be expressed as a function of time t or other covariates:

$$f(x) = \frac{\beta(t)^{\alpha(t)}}{\Gamma(\alpha(t))}(x_t - r(t))^{\alpha(t)-1}e^{-\beta(t)(x_t-r(t))} \tag{3}$$

In this study, the shape parameter $\alpha(t) = \exp\{k_0 + k_1 t + k_2 t^2\}$, scale parameter $\beta(t) = \exp\{k_3 + k_4 t + k_5 t^2\}$, and location parameter $r(t) = \exp\{k_6 + k_7 t + k_8 t^2\}$ are exponential functions related to time t. The using of the exponential function is to ensure that the positivity of α and β are respected for all values of t.

By changing the value of $k_i (i = 0, 1, \cdots, 8)$, there are 27 models in which the exponential functions are constant, linear or quadratic. The models with time dependence of order i in the shape parameter, order j in the scale parameter and order k in the location parameter are denoted by M_{ijk} ($i = 0, 1, 2$; $j = 0, 1, 2$; $k = 0, 1, 2$) (some examples are presented in Table 1). For example, M_{012} indicates a model that the shape parameter is independent of time, while the scale parameter and location parameter has a linear and quadratic trend, respectively. Besides, $k_i (i = 0, 1, \cdots, 8)$ is the parameter of trend functions, i.e., the parameters to be estimated are $\{k_0; k_3, k_4; k_6, k_7, k_8\}$ for the M_{012} model, $\{k_0, k_1; k_3, k_4; k_6, k_7\}$ for the M_{111} model.

Table 1
Examples of Pearson type 3 distribution with time-varying parameters.

$k_i$values	Exponential functions of time-varying parameters		
	$\alpha(t)$	$\beta(t)$	$r(t)$
$k_0 \neq 0,\ k_1 = 0,\ k_2 = 0$ $k_3 \neq 0,\ k_4 = 0,\ k_5 = 0$ $k_6 \neq 0,\ k_7 = 0,\ k_8 = 0$	Constant	Constant	Constant
$k_0 \neq 0,\ k_1 \neq 0,\ k_2 = 0$ $k_3 \neq 0,\ k_4 = 0,\ k_5 = 0$ $k_6 \neq 0,\ k_7 = 0,\ k_8 = 0$	Linear	Constant	Constant
$k_0 \neq 0,\ k_1 = 0,\ k_2 = 0$ $k_3 \neq 0,\ k_4 \neq 0,\ k_5 = 0$ $k_6 \neq 0,\ k_7 = 0,\ k_8 = 0$	Constant	Linear	Constant
$k_0 \neq 0,\ k_1 = 0,\ k_2 = 0$ $k_3 \neq 0,\ k_4 = 0,\ k_5 = 0$ $k_6 \neq 0,\ k_7 \neq 0,\ k_8 = 0$	Constant	Constant	Linear
$k_0 \neq 0,\ k_1 = 0,\ k_2 = 0$ $k_3 \neq 0,\ k_4 \neq 0,\ k_5 = 0$ $k_6 \neq 0,\ k_7 \neq 0,\ k_8 \neq 0$	Constant	Linear	Quadratic

2.1.2. Parameter estimation

Assuming $X_1, X_2, \cdots, X_n$ is a sequence of hydrological variables that are distributed within the nonstationary P3 distribution. Under the nonstationary condition, we can have the likelihood estimators of $X_1, X_2, \cdots, X_n$

$$L(\alpha(t), \beta(t), r(t)) = \prod_{t=1}^{n} \frac{\beta(t)^{\alpha(t)}}{\Gamma(\alpha(t))}(x_t - r(t))^{\alpha(t)-1} e^{-\beta(t)(x_t - r(t))} \tag{4}$$

It is more convenient to take logarithms of Eq. (4) and have the log-likelihood estimators

$$D = \ln[L(\alpha(t), \beta(t), r(t))] = \sum_{t=1}^{n} \ln\left(\frac{\beta(t)^{\alpha(t)}}{\Gamma(\alpha(t))}(x_t - r(t))^{\alpha(t)-1} e^{-\beta(t)(x_t - r(t))}\right) \tag{5}$$

By using a Nelder-Mead or Newton-Raphson algorithm, it can obtain the maximum likelihood estimators $\hat{\alpha}(t)$, $\hat{\beta}(t)$, $\hat{r}(t)$ of parameters. As the P3 distribution has a lower bound at the location parameter, the likelihood is not derivable for the location parameter, and the maximum likelihood estimator of the location parameter is actually the first order statistic of the sample. This can also provide a reference when using numerical techniques to obtain the maximum likelihood estimators.

Unlike the stationary P3 distribution, there are some drawbacks when using MLE method to estimate the nonstationary P3 distribution parameters. For instance, the changes of location parameters $r(t)$ in a nonstationary model may lead to a result of $(x_t - r(t)) \approx 0$, which can generate unreasonable likelihood value, exerting a significant impact on the optimization progress, no matter what kind of algorithms are used in the MLE method. For example, the probability density obtained from Eq (3) should lie between 0 and 1, and Eq (5) will generate a negative log-likelihood value. In the case of $(x_t - r(t)) \approx 0$ and shape parameter $\alpha < 1$, Eq (3) will frequently generate comparatively large values (i.e., $\times 10^6$), resulting in a positive value from the log-likelihood function. Moreover, Eq (3) may also return a complex number when $(x_t - r(t)) \approx 0$. The optimization process is disturbed by these problems, which will doubt the precision of parameter estimation. A penalized term $\pi(x_t - r(t))$ is introduced in the optimization process to avoid such problems. It is defined as:

$$\pi(x_t - r(t)) = \begin{cases} 1 & (x_t - r(t) > B) \\ \exp\{[a \cdot (x_t - r(t) - B)]^c\} & (x_t - r(t) \leqslant B) \end{cases} \quad (t = 1, 2, \ldots, n) \tag{6}$$

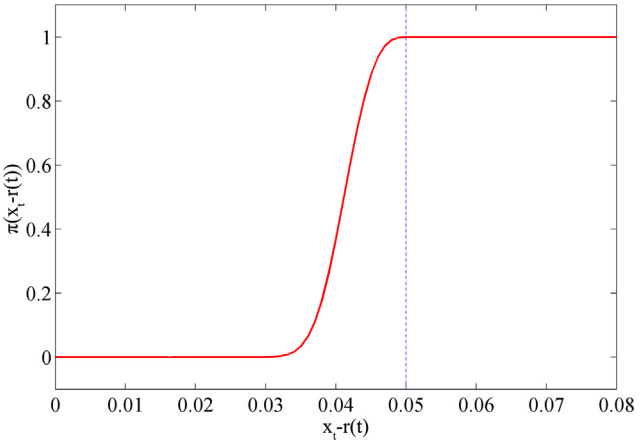

Fig. 1. Penalty function for the probability density function of the nonstationary P3 model.

where the coefficients are set as $a = 100$, $c = 3$ and $B = 0.05$ in this study. A small value of B means a more restrictive penalty on location parameter r. The a and c values indicate the convergence rate, and the large values of them are corresponding to a small interval from $\pi(x - r) = 1$ to $\pi(x - r) = 0$. Fig. 1 shows the penalty function $\pi(x - r)$ with coefficients $a = 100$, $c = 3$ and $B = 0.05$.

Each of the observations x_t has a corresponding probability density $f(x_t;\ \alpha(t), \beta(t), r(t))$, which is penalized by the corresponding $\pi(x_t - r(t))$. If the location parameter is a constant value, the penalty function is actually based on the difference between x_1 and r, in which x_1 is the minimum value of data series. The likelihood function $L(\alpha(t), \beta(t), r(t))$ is transformed into a penalized likelihood function $\prod_{t=1}^{n}[f(x_t) \cdot \pi(x_t - r(t))]$. The penalized log-likelihood function equals the expression in (5) plus $\ln[\pi(x_t - r(t))]$, which is:

$$D = \ln[L(\alpha(t), \beta(t), r(t))] + \ln[\pi(x_t - r(t))] \tag{7}$$

The parameters of the nonstationary P3 model can be obtained by maximizing the log-likelihood function in Eq. (7).

2.2. Nonstationary GEV model

The GEV distribution is the combination of continuous probability distributions including the Gumbel, Fréchet, and Weibull families (Jenkinson, 1956). Under the nonstationary condition, the GEV distribution has a cumulative distribution function:

$$F(x) = \begin{cases} \exp\{-[1 + \xi(t)\frac{(x-\mu(t))}{\sigma(t)}]^{-1/\xi(t)}\} & \xi(t) \neq 0 \\ \exp\{-\exp[-\frac{(x-\mu(t))}{\sigma(t)}]\} & \xi(t) = 0 \end{cases} \tag{8}$$

where $1 + \xi(t)(x - \mu(t))/\sigma(t) > 0$, $\mu(t) \in R$, $\sigma(t) > 0$ and $\xi(t) \in R$ are the location, scale and shape parameters, respectively.

The GEV distribution has been widely used in the hydrological frequency analysis. By considering a linear or quadratic dependence on covariates, the GEV models with time dependence of order i in the scale parameter and order j in the location parameter are denoted by GEV_{ij} ($i = 0, 1, 2, 3$; $j = 0, 1, 2, 3$). The maximum likelihood estimation (MLE) method is the most popular method for the development of computer sciences. However, Hosking et al. (1985) pointed that the L-moments estimation was superior to the MLE method for sample sizes varying from 15 to 100. Moreover, previous studies found that the MLE may generate absurd values of the shape parameter, especially for the small samples (record length < 50). However, the L-moments can only be used under the stationary assumption, which largely restricted its application. Then, several methods were proposed to improve the performance of MLE method. Coles and Dixon (1999) proposed a penalized MLE method to restrict the value of shape parameter. Martins

and Stedinger (2000) proposed a generalized maximum likelihood estimation (GMLE), which could provide a more restrictive penalty on the shape parameter. Morrison and Smith (2002) developed a mixed method, which combined the MLE and L-moments method, to avoid the problems mentioned above. The GMLE method was widely used and further developed in a nonstationary condition (Adlouni et al., 2007; Cannon, 2010). The generalized likelihood function is defined as:

$$\ell_{GL} = \pi(\xi)\cdot L_n \tag{9}$$

$$L_n = \prod_{t=1}^{n} f(x_t; u_t, \sigma_t, \xi_t) \tag{10}$$

where L_n is the likelihood function of sample series (details can be seen in Martins and Stedinger, 2000), the penalized function $\pi(\xi)$ is the beta distribution given by $\pi(\xi) = (0.5 + \theta_3)^{p-1}(0.5 - \theta_3)^{q-1}/B(p, q)$ with $p = 6$ and $q = 9$, wherein $B(p, q) = \Gamma(p)\Gamma(q)/\Gamma(p + q)$.

2.3. Model checking

The commonly used methods, Akaike Information Criterion (AIC) and Bayesian Information Criterion (BIC) are introduced in this paper to compare the performance of different models. These statistics are given by:

$$AIC = -2LLF + 2numPar \tag{11}$$

$$BIC = -2LLF + numPar \times \log(n) \tag{12}$$

where LLF is the maximized log-likelihood, $numPar$ is the number of parameters, and n is the record length. A lower value of AIC or BIC indicates a better model. In the simulation study, the best model is determined by the AIC and BIC values, and the root mean square error (RMSE) is computed for different quantiles (non-exceedance probabilities p = 0.5, 0.8, 0.9, 0.95, 0.99) with sample sizes n = 20, n = 40, n = 60, n = 80, n = 100.

2.4. Methods of uncertainty analysis

The profile likelihood method is assumed to be a robust and accurate method in uncertainty analysis for extreme events (Coles, 2001; Obeysekera and Salas, 2014; Serinaldi and Kilsby, 2015). Based on the asymptotic properties of maximum likelihood estimators, the profile method can be used to estimate the confidence intervals with the following steps:

The fitted P3 distribution has a parameter vector $(\theta|\alpha, \beta, r)$, and the quantile Q_p with nonexceedance probability p $(0 < p < 1)$ is obtained as

$$Q_p = gaminv\left(p, \alpha, \frac{1}{\beta}\right) + r \tag{13}$$

where *gaminv* is the Gamma inverse cumulative distribution function.

Let θ_i denotes a particular parameter which is desired to estimate its confidence interval, and θ_{-i} is the remaining parameters in θ. The shape parameter of P3 distribution is set to be the particular parameter because it can affect the type of distribution (Buckett and Oliver, 1977). The profile log-likelihood for θ_i is defined as (Coles, 2001)

$$\ell_p(\theta_i) = \max_{\theta_{-i}} \ell(\theta_i, \theta_{-i}) \tag{14}$$

Eq. (14) is used to obtain the maximum value concerning all parameters expect θ_i. The approximation of a $(1 - \alpha)$ confidence interval of θ_i is computed as

$$\{\theta_i: 2(\ell(\hat{\theta}) - \max \ell_p(\theta_i)) \leqslant c_{1-\alpha}\} \tag{15}$$

where $\ell(\hat{\theta})$ is the corresponding log-likelihood values of θ, and $c_{1-\alpha}$ is $(1 - \alpha)$ quantile of the Chi-square distribution with one degree of freedom.

By introducing the design quantile Q_p into the likelihood function, the location parameter can be obtained from Eq. (9), as follows

$$r = Q_p - gaminv\left(p, \alpha, \frac{1}{\beta}\right) \tag{16}$$

After reparameterization (Q_p, α, β), it can obtain the log-likelihood estimators based on Eq. (7). According to Eqs. (7) and (15), the corresponding confidence intervals for the design quantile can be efficiently calculated by substituting different Q_p values into the reparameterized distribution $f(x|Q_p, \alpha, \beta)$. The preceding steps can be easily implemented under the stationary condition, while Q_p has the same record length with the sample under the nonstationary case. Assuming that the shape parameter α is a constant value, we maximize Eq. (7) with respect to the remaining parameters, and repeat this step in a certain range of α. Then, we can have a set of the maximum likelihood estimates $(\hat{\alpha}, \hat{\beta}, \hat{r})$. Different Q_p values are computed based on $(\hat{\alpha}, \hat{\beta}, \hat{r})$, and the corresponding confidence intervals for a design quantile can be computed by substituting different Q_p values into equations.

3. Selection of time-varying parameters

The changing parameters influence the nonstationary P3 distribution model. The effects of shape, scale and location parameters are investigated before the analysis, which can provide a reference for identifying the suitable parameter that shows nonstationarity in the nonstationary model. For example, the location parameter and scale parameter in GEV distribution are approximate to the mean value and variance, respectively. Both parameters are likely to consider as the time-varying parameters, while the shape parameter indicates the distribution families, and is commonly supposed to be stationary in previous studies (Adlouni et al., 2007; Panagoulia et al., 2014). To our knowledge, the selection of time-varying parameters in a nonstationary P3 model was never discussed before, and we hope the following discussion may be helpful to choose the proper model structure.

We collected discharge records for a 52-year period from the Miyun Reservoir, and the annual runoff time series is used as the sample series to study the effects of different parameters on the P3 model. By using the stationary P3 model, the shape, scale, and location parameters are 1.672, 0.223 and 1.566, respectively. We change the value of a single parameter while holding others constant to analyze the effect of each parameter. Buckett and Oliver (1977) indicated that the shape parameter α affected the form of probability density function (Fig. 2). It can improve the model performance by considering trends in the shape parameter. The AIC and BIC values of the model M_{100} are 287.45 and 295.25, respectively, which are comparatively small to that of the stationary P3 model (312.24 and 318.09, respectively). The location parameter r is mainly influencing the upper bounds of the probability density function (Fig. 2); it is related to the mean value of the sample and is most likely to be dependent on covariates. The scale parameter β is expected to affect tail behaviors (Fig. 3). A large value of β generally indicates a heavy-tailed case, while the small β means a light-tailed or short-tailed distribution. In all the cases, the nonstationary P3 model can better explain the variation in data for the sample series with a significant trend. Further analysis is conducted in the simulation study, and all of the three parameters are time-dependent for the nonstationary P3 model in this study.

4. Simulation study

To compare the performance of the two nonstationary models, the Monte Carlo simulation was adopted to generate samples following GEV_{01} $(\mu = -0.1t + 20, \sigma = 5, \xi = 0.1)$, GEV_{10} $(\mu = 20, \sigma = -0.025t + 5, \xi = 0.1)$, and GEV_{11} $(\mu = -0.1t + 20, \sigma = -0.025t + 5, \xi = 0.1)$ models. The influences of sample sizes were considered by using five scenarios (record length n = 20, 40, 60, 80 100); we

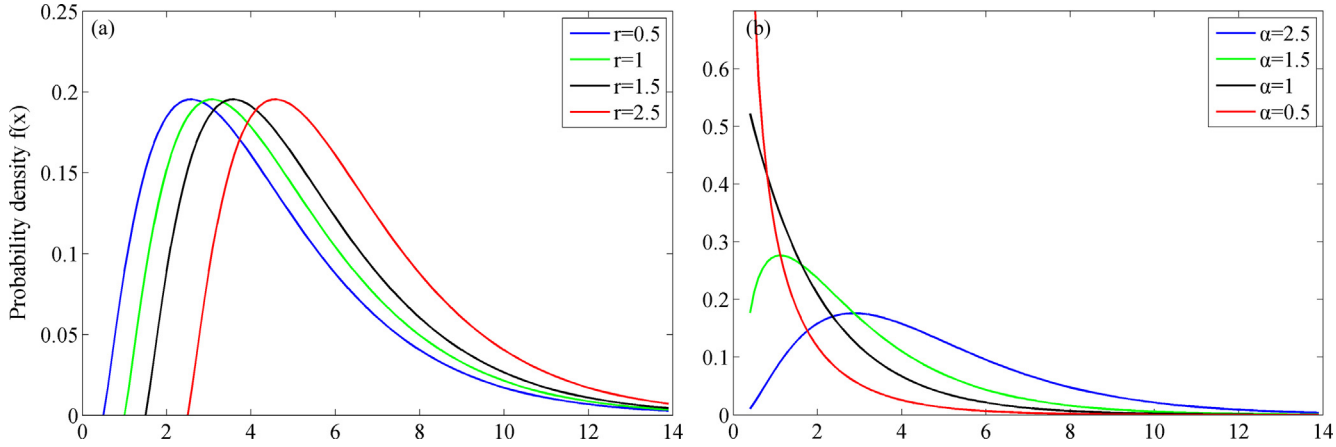

Fig. 2. The effects of location and shape parameters on the sampling frequency ((a) Location parameter; (b) Scale parameter).

generated 10,000 samples for each of the five scenarios.

In the simulation study, The GMLE method and MLE method were used to estimate the parameters of the nonstationary GEV models. The model with the lower bias was compared to the nonstationary P3 model, and the GMLE method outperformed the MLE method in most cases. For samples obtained from GEV_{01} and GEV_{10} models, we considered linear (M_{001}, M_{010}, M_{100}) variations in a single parameter of the P3 model to fit the simulated samples. For samples obtained from the GEV_{11} model, there were 4 alternative P3 models, including M_{011}, M_{101}, M_{110}, and M_{111}. The best of these models was compared to the corresponding GEV model.

Table 2 presents the RMSE of different quantiles obtained with the nonstationary GEV models and the best of P3 models. For small samples (n = 20 and n = 40), the nonstationary P3 model performs much better than the nonstationary GEV model. The difference reduces significantly with the increase in sample sizes because more information is available. For quantiles with low probabilities of non-exceedance, the result of the GEV model is similar to that of the P3 model, whereas the GEV model leads to high biases for quantiles with high non-exceedance probability. Exceptions can be detected from samples obtained from the GEV_{10} model, in which the GEV model has outperformed the best of P3 model when there is a large sample size (n ≥ 80). These exceptions may be caused by the difference between both models; the GEV_{10} model only considers temporal evolutions in scale parameter, and the samples generated by it may hardly be described by the P3 model.

By using samples generated by the GEV_{11} model, Fig. 4 shows a boxplot of RMSE for each quantile obtained with GEV and P3 models. Similar to the results displayed in Table 2, significant differences are noted with changes in sample sizes. The nonstationary P3 model dramatically reduces the model uncertainties for small samples and quantiles with high non-exceedance probability.

Based on the samples obtained from GEV models, we can further analyze the model structures under nonstationary condition. Table 3 presents the results that which P3 model is suitable for samples generated by different GEV models. For high non-exceedance probability, we can infer that the model structure is highly related to the GEV model which has been used to generate samples, especially for a large sample. Besides, the location parameter is most likely to be time dependent in a nonstationary P3 model. However, this conclusion is only valid in estimating design value with high quantiles. For quantile = 0.5, the performances of M_{001}, M_{010}, and M_{100} are slightly different from each other. Considering that the main objective is to estimate the frequency of extreme events, these results are not presented in this paper.

5. Applications

5.1. Case of nonstationary time series

The rapid urbanization increases demand for water, resulting in a decreasing trend in groundwater as well as surface runoff. On the other hand, urban flood hazard, which is mainly caused by the extreme precipitation, is even more severe in recent years. The linear regression and Mann-Kendall methods are used to analyze the trend. The discharge records were collected for a 52-year period in the Miyun Reservoir, which is one of the most critical water supply sources in Beijing (Fig. 5). Flood records of the Wangkuai reservoir were provided by the Haihe River Water Conservancy Commission (Fig. 5). The annual maximum daily precipitation time series were collected from 8

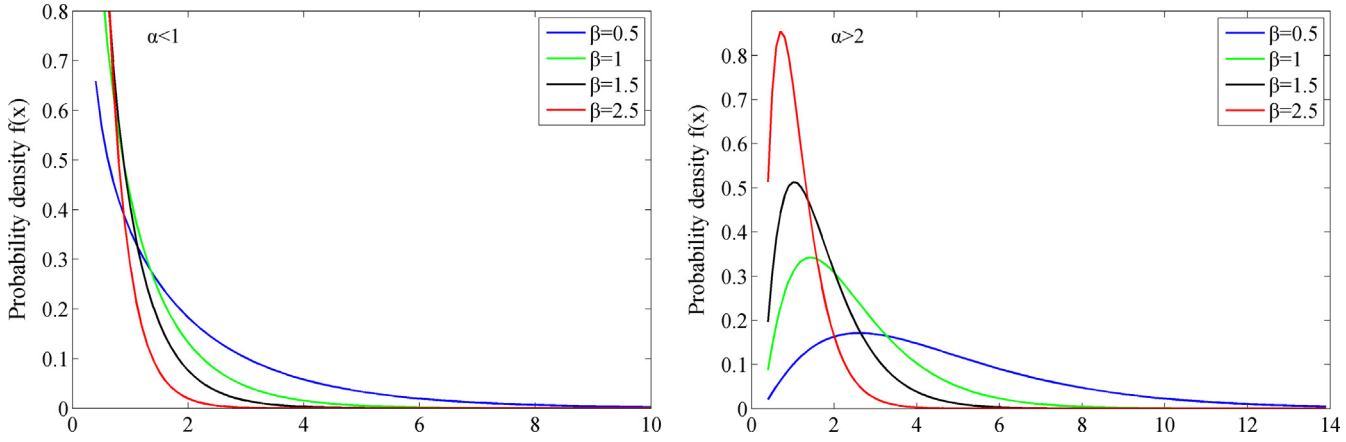

Fig. 3. The effects of scale parameter on the sampling frequency based on two cases (shape parameter $\alpha < 1$ and $\alpha > 1$).

Table 2
RMSE of quantiles estimated by the GEV and P3 models.

Samples	Quantile	n = 20		n = 40		n = 60		n = 80		n = 100	
		P3	GEV	P3	GEV	P3	GEV	P3	GEV	P3	GEV
Generated by GEV_{01}	0.99	7.170	14.56	6.898	10.29	6.935	8.170	6.856	7.173	6.440	6.679
	0.95	3.852	5.212	3.148	3.883	2.895	3.319	2.743	3.009	2.628	2.832
	0.9	2.818	3.284	2.149	2.394	1.877	2.075	1.739	1.887	1.693	1.769
	0.8	2.043	2.271	1.473	1.575	1.226	1.329	1.099	1.184	1.063	1.084
	0.5	1.456	1.784	1.013	1.188	0.815	0.952	0.729	0.812	0.722	0.719
Generated by GEV_{10}	0.99	6.880	17.38	6.563	10.64	6.617	7.713	6.659	6.253	6.690	5.388
	0.95	3.673	6.860	3.041	4.251	2.904	3.233	2.868	2.675	2.882	2.313
	0.9	2.666	4.323	2.058	2.643	1.874	2.021	1.804	1.669	1.789	1.434
	0.8	1.914	2.687	1.376	1.609	1.175	1.206	1.081	0.975	1.028	0.820
	0.5	1.348	1.475	0.914	0.871	0.701	0.614	0.569	0.475	0.472	0.384
Generated by GEV_{11}	0.99	6.818	16.79	6.234	10.53	6.037	7.818	5.795	6.292	5.532	5.496
	0.95	3.795	6.810	3.059	4.383	2.683	3.406	2.425	2.789	2.252	2.430
	0.9	2.789	4.427	2.146	2.836	1.793	2.215	1.570	1.815	1.422	1.563
	0.8	2.038	2.907	1.499	1.840	1.202	1.422	1.037	1.149	0.931	0.970
	0.5	1.517	1.848	1.011	1.151	0.777	0.849	0.673	0.688	0.635	0.570

meteorological stations, in which some places have suffered severe urban flood inundation in recent years (Fig. 5). The results of trend analysis show that the trends of those sample series are statistically significant ($P < 0.05$, Figs. 6 and 7). The nonstationarity in hydrological events may be caused by climate change or human activities. However, the traditional statistical methods assume that the hydrological events are stationary. To have a precise quantile estimation under nonstationary conditions, we consider a nonstationary P3 model in which the parameters are time-dependent. The parameter can also be dependent on other covariates (i.e., climate indicators) if the physical mechanism for hydro-meteorological patterns has been thoroughly investigated. Human activities can also be considered as covariates, as previous studies also reported that the reservoir operation had great potential to control flood and cause intra-annual runoff alteration (Seibert et al., 2014; Lin et al., 2017).

5.2. Case studies

5.2.1. Decreasing discharges

In this section, all the parameters are assumed to be time-dependent in the nonstationary P3 model, while the nonstationary GEV model considers changes in scale and location parameters. Table 4 shows the performance of different models, in which we only present the results of nonstationary models that are less biased. The annual runoff time series and flood records have significant trends, so the results of stationary models are highly biased. In comparison, the nonstationary model can generate comparatively precise results. Results also show that the P3 model is superior to the GEV model in both stationary and nonstationary cases. For the annual runoff time series, the M_{001} model has the minimum values of AIC and BIC (284.62 and 292.43, respectively), indicating a linear dependence of the location parameter on time. In general, the BIC penalizes complex models more strongly than the AIC (Panagoulia et al., 2014); this explains that the M_{201} and M_{102} models have small AIC values and relatively large BIC values (Table 4).

Based on the fitted P3 model, Fig. 8 shows the variations of probability density function. As the data series has a decreasing trend during the past decades, the small value is going to have a large probability density with the changing parameter. The applied functions are highly depending on the statistical characteristics of the sample because time t is selected as the covariate in the nonstationary model, which means a lack of understanding the physical mechanisms of the relationship between runoff and covariate. In this study, the annual runoff time series have a monotonic trend; unlike the samples that fluctuate frequently, therefore, it can be described by a simple function. For example, the M_{002} model (AIC = 286.78, BIC = 296.54) is not able to perform better than the M_{001} model. The results of GEV models can also approve this point. On the contrary, the temporal evolution of annual maximum daily discharges is more drastic. In consequence, the complex model can generate more accurate results; the M_{020} model (BIC = 362.13) performs much better than the M_{010} model (BIC = 369.51). Besides, it should be noticed that polynomial functions may not well describe variations in samples. In general, a suitable and complex function can lead to less biased results, i.e., cubic spline can highlight non-linear dependencies in flood properties over time (Villarini et al., 2009).

5.2.2. Increasing extreme rainfall

With the rapid urbanization, many studies indicated that the extreme rainfall exhibited an increasing trend in the urban region, which could be necessary for the urban drainage network design (De et al., 2009). There is a need to consider nonstationarity in the probability distribution of extreme rainfall. We applied nonstationary P3 and GEV models to annual maximum daily precipitation series, in which significant increasing trends can be detected. Previous studies indicated that the record lengths could affect the performance of estimation methods. As a result, the data series were collected from 8 meteorological stations and with different record lengths (from 25 years to 61 years, Fig. 5). The parameters and model diagnostics of GEV and P3 models were calculated by using the methods presented in Section 2.

As there are eight stations, this section only shows the best P3 and GEV models for each station (Table 5). Except for the Shanghai station, the results apparently indicate that the nonstationary P3 model can explain a substantial amount of the variation in the data. The nonstationary GEV model is equally efficient to the nonstationary P3 model in the Yicheng station, which has short sample series, indicating the superiority of GMLE method in small samples. The above discussions are also proved by Table 5: the nonstationary GEV model can better explain the variation in data by considering the trends in location and scale parameters. The P3 models with a time-varying location parameter are recommended for the Xiamen and Banga stations, while for the Shanghai, Qiongshan and Wenchang stations, the shape parameter of the best models are dependent on time.

5.2.3. Uncertainty analysis

We use the annual runoff series in the Miyun reservoir to illustrate the application of the profile likelihood method. Based upon the above analysis, the M_{001} model is more suitable to represent data than others according to the model diagnostic. To observe the difference between those models, we compute the return levels estimated by the M_{000}, and M_{001} models. The corresponding confidence intervals are computed by the profile likelihood method, and the results are presented in Fig. 9.

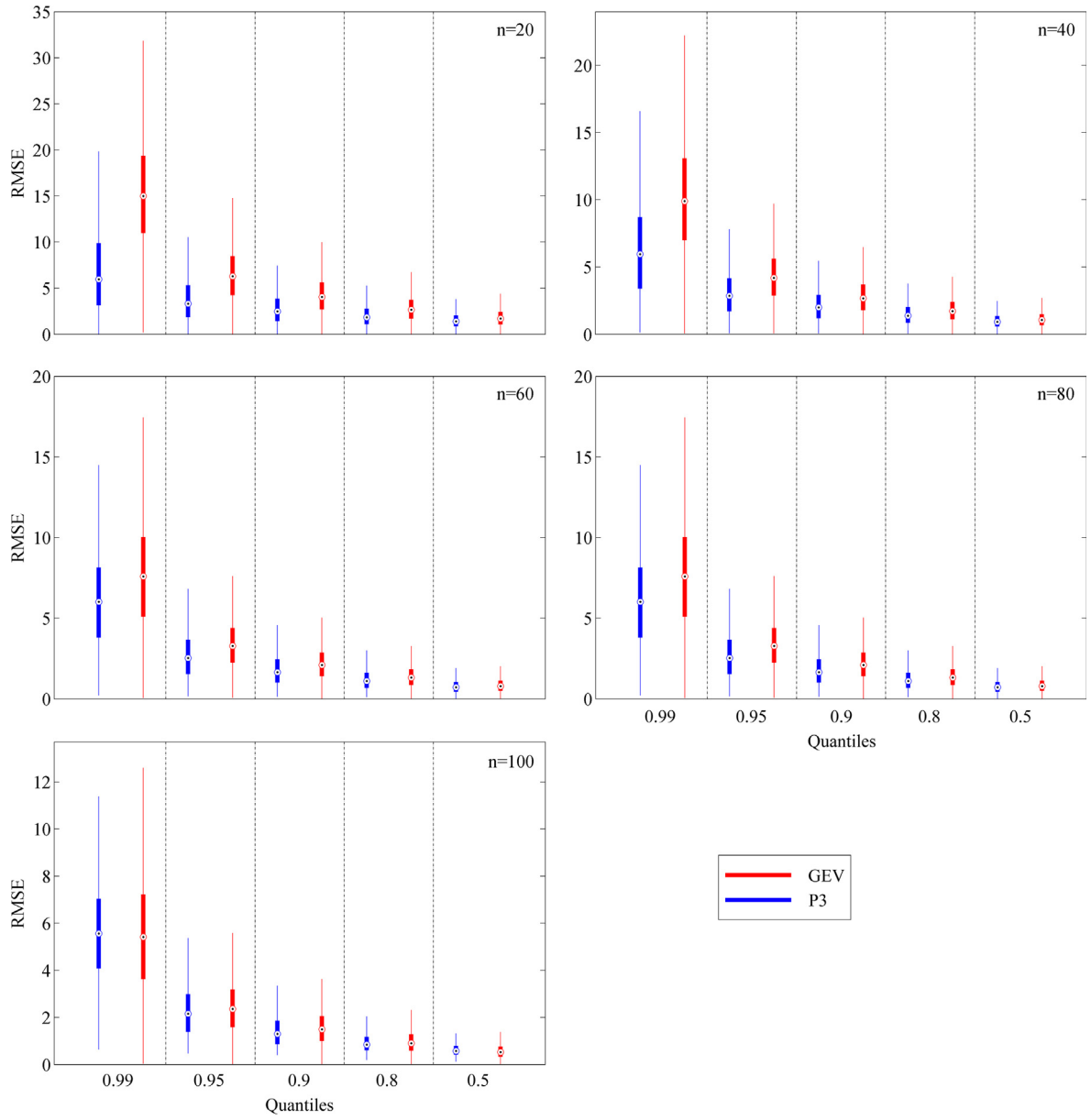

Fig. 4. Box plot of RMSE of non-exceedance probability quantiles at sample sizes n = 20, 40, 60, 80, 100. The plot shows the median, inter-quartile range (box) and whiskers; the outliers have been removed in this plot.

Table 3
Performance of nonstationary P3 models (results are displayed in percentage, i.e., for n = 20 and quantile = 0.99, 61.8% of the 10,000 samples are fitted by the M_{001} model to achieve the most accurate result).

Samples	Sample size	Quantile = 0.99			Quantile = 0.95		
		M_{001}	M_{010}	M_{100}	M_{001}	M_{010}	M_{100}
Generated by GEV_{01}	20	61.80%	16.20%	22.00%	60.10%	21.33%	18.57%
	40	72.95%	6.69%	20.36%	69.54%	10.61%	19.85%
	60	80.78%	2.77%	16.45%	76.66%	6.46%	16.88%
	80	89.88%	0.71%	9.41%	84.65%	3.32%	12.03%
	100	96.31%	0.19%	3.50%	88.20%	1.85%	9.95%
Generated by GEV_{10}	20	60.92%	18.29%	20.79%	58.95%	22.60%	18.45%
	40	66.38%	17.91%	15.71%	58.76%	23.79%	17.45%
	60	55.47%	34.58%	9.95%	37.39%	48.07%	14.54%
	80	40.55%	56.22%	3.23%	19.71%	74.28%	6.01%
	100	27.50%	71.72%	0.78%	7.60%	91.03%	1.37%

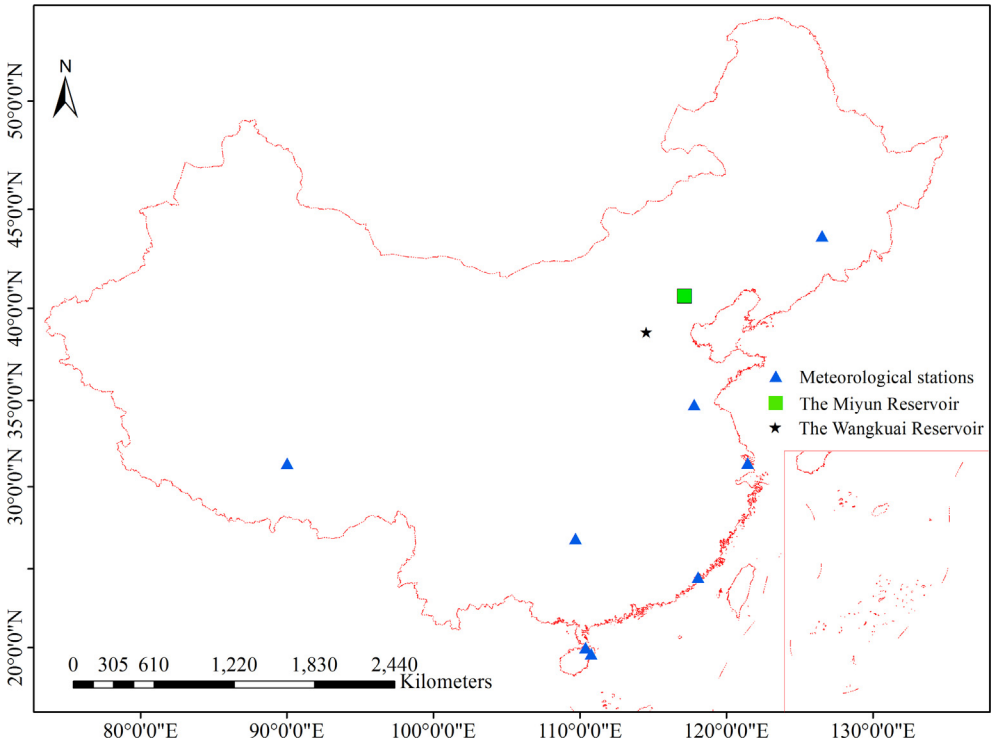

Fig. 5. Location of the reservoir and meteorological stations.

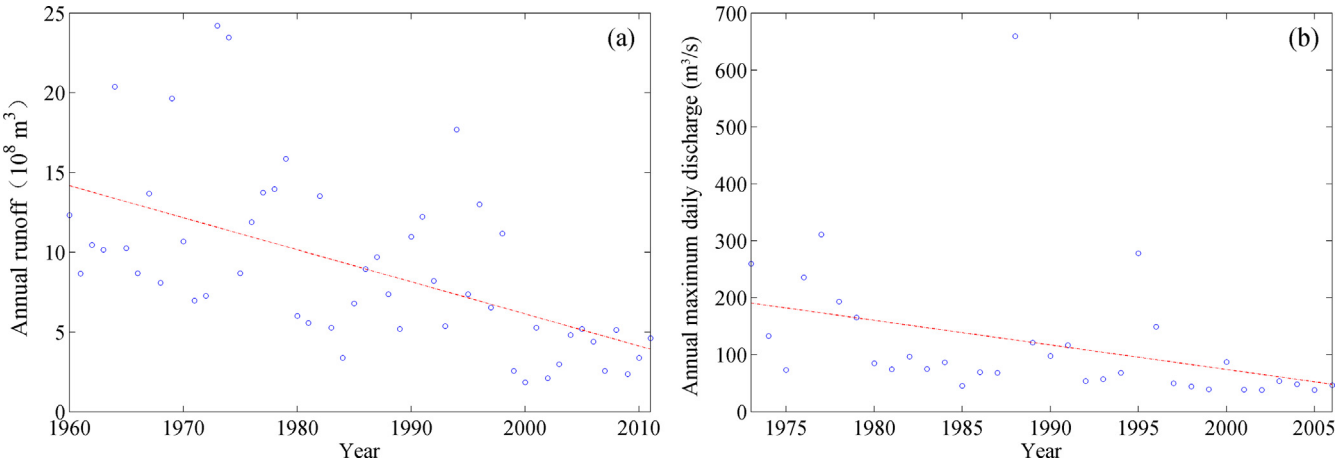

Fig. 6. Temporal changes of annual runoff and annual maximum daily discharges. ((a) Miyun reservoir, 1960–2011; (b) Wangkuai reservoir 1973 – 2006).

The estimates of quantiles given by the M_{001} model show steadily decreasing trends, which is similar to that of the annual runoff series. As a large design value is generally corresponding to high uncertainty, the confidence intervals are clearly asymmetric under stationary and nonstationary conditions. Although the profile likelihood method can be used in this case, there is a problem that should be noticed before using this method. As we mentioned before, the parameters are redefined as (Q_p, α, β), and we can have the location parameter according to the Eq. (16). In general, we should substitute large Q_p values into equations to estimate the upper limit of the confidence interval, but this process can also lead to large values of location parameter r, which inevitably results in negative values of $(x - r)$. As a result, the numerical technique may fail to generate optimal results because the initial value of r is too absurd. As the *gaminv* function is monotonically increased with the decrease of scale parameter β ($\beta > 0$), this problem can be avoided by changing the initial value of β. For the nonstationary P3 distribution, the profile likelihood method should be further studied in the future. Besides, bootstrap methods can also give a realistic estimation for uncertainties, at least for the GEV distribution (Serinaldi and Kilsby, 2015), and it can be considered in future studies.

Table 6 presents more details of return levels for the following periods: 1960–1970, 1971–1980, 1981–1990, 1991–2000, and 2001–2011. The results show that the return levels given by the M_{001} model have a significant inter-annual difference. Indeed, the estimated values in the 1960–1970 period can be 6×10^8 m^3 higher than that in the 2001–2011 period. Therefore, the use of an improper model (i.e., stationary model or nonstationary models without proper consideration for the parameters) can result in a significant overestimation or underestimation of the return levels.

6. Summary and conclusion

This study presented a nonstationary P3 model which can be used efficiently to describe the variance in data. The nonstationarity in data

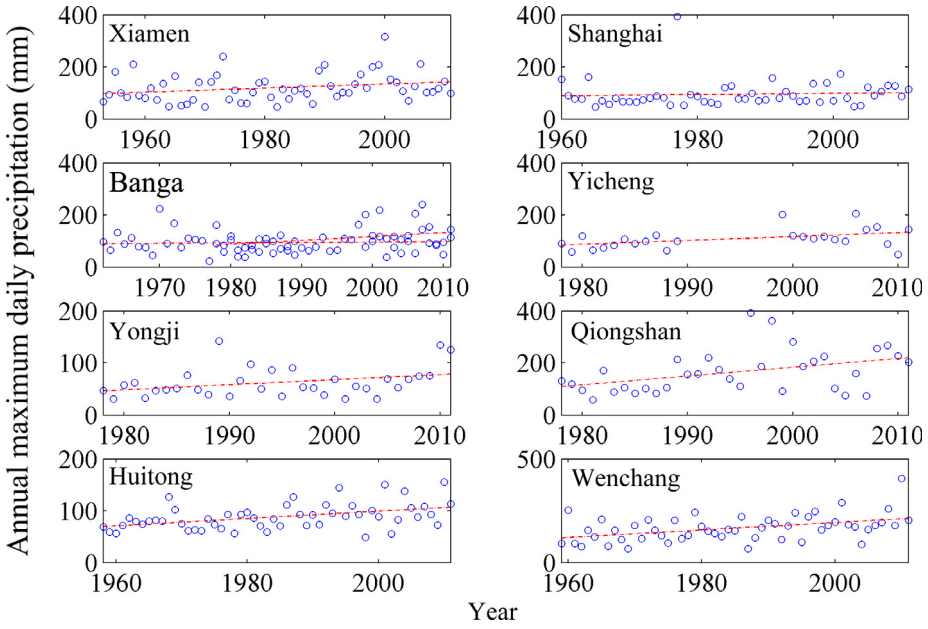

Fig. 7. Temporal changes of annual maximum daily precipitation in the meteorological stations.

Table 4
The performance of different P3 and GEV models.

Data	Models	AIC	BIC	Models	AIC	BIC
Annual runoff (Miyun Reservoir)	M_{000}	312.24	318.09	GEV_{00}	315.28	321.14
	M_{001}	284.62	**292.43**	GEV_{01}	286.75	294.56
	M_{002}	286.78	296.54	GEV_{02}	293.25	303
	M_{201}	**284.49**	296.2	GEV_{11}	287.17	296.92
Flood (Wangkuai Reservoir)	M_{000}	362.51	367.09	GEV_{00}	373.65	378.23
	M_{100}	347.86	**353.97**	GEV_{01}	365.75	371.86
	M_{021}	348.50	357.66	GEV_{11}	354.82	362.46
	M_{102}	**347.35**	356.51	GEV_{12}	355.89	365.05

was analyzed using time-varying parameters in the P3 model. To verify the performance of the P3 model in modeling hydrological events, the results of the P3 model were compared to that obtained from the GEV model, which was widely accepted to describe the nonstationarity. The nonstationary GEV model only considers the trends in location and scale parameters.

The MLE method is used in parameter estimation for those models. However, the maximum likelihood estimators of the GEV model may generate a significant variance for small samples, and the MLE method may result in unreasonable results when used to estimate the parameters of a nonstationary P3 model. For the nonstationary P3 model, we added a penalized term to the likelihood function, in which the location parameter is restricted according to the sample variables. The P3 model is rarely used in the nonstationary condition, so its estimation methods can be further developed in the future studies. The penalized term provided in this paper has a major drawback that it arbitrarily overlooks some model outputs if the location parameter cannot meet the requirements $(x - r) > 0.05$. Thus, there are significant rooms for improving the performance of the nonstationary P3 model by using modified MLE method.

A special case, which is rarely occurred in natural conditions, can significantly affect the performance of P3 distribution. This is necessary to be mentioned when estimating the parameters of the nonstationary P3 distribution based on the PMLE method. For example, the annual maximum/minimum series $x_{1,2,\ldots,n}$ has a very large maximum value (i.e., $x_{t1} = 1000$) when compared to its minimum value (i.e., $x_{t2} = 10$). To have a precise estimation, in this case, we should assure that the $(x - r)$ values are reasonable at t_1 and t_2. Therefore, the parameters

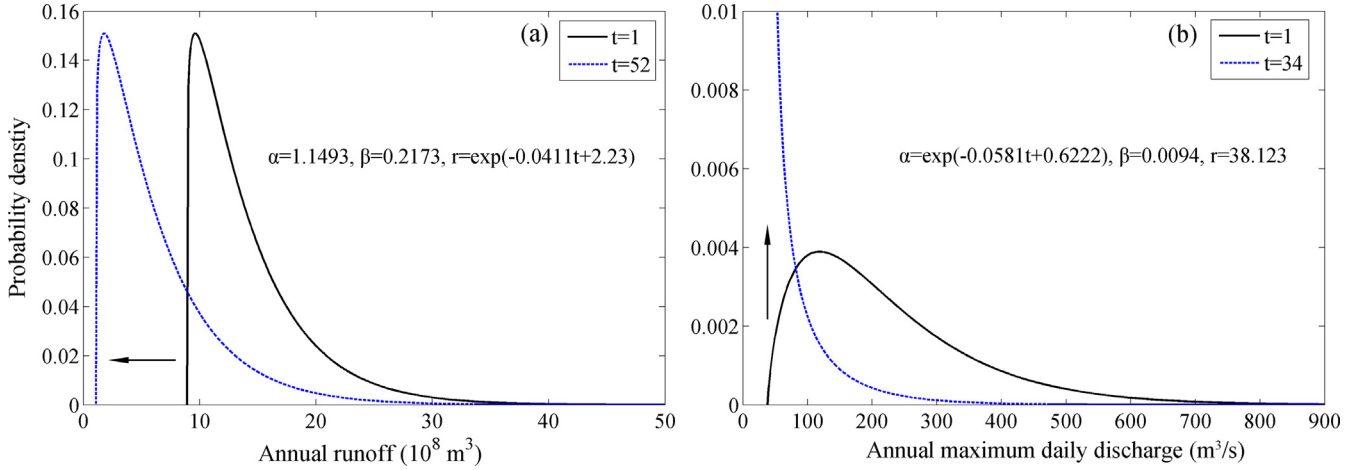

Fig. 8. Variations of the probability density function in the nonstationary P3 distribution. ((a) M_{001} model, annual runoff series; (b) M_{100} model, annual maximum discharge).

Table 5
The performance of best P3 and GEV models in each station.

Station	Record lengths (years)	Models	AIC	BIC	Models	AIC	BIC
Xiamen	1950–2011 (61)	GEV_{01}	648.88	657.32	M_{002}	645.52	653.96
Shanghai	1951–2011 (60)	GEV_{01}	586.63	595.00	M_{100}	588.56	596.94
Banga	1956–2011 (55)	GEV_{11}	339.96	350.00	M_{101}	336.54	346.58
Yicheng	1986–2011 (25)	GEV_{11}	252.65	258.75	M_{010}	252.98	257.85
Yongji	1977–2011 (34)	GEV_{11}	313.72	321.35	M_{010}	309.25	315.35
Qiongshan	1977–2011 (34)	GEV_{11}	387.50	395.13	M_{200}	384.70	392.34
Huitong	1957–2011 (54)	GEV_{11}	484.67	494.61	M_{010}	484.77	492.73
Wenchang	1958–2011 (53)	GEV_{01}	580.01	587.89	M_{100}	578.01	585.89

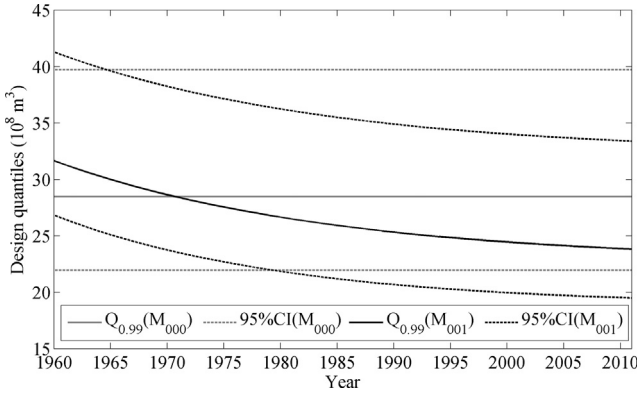

Fig. 9. Return levels of annual runoff in the Miyun reservoir, obtained by stationary and nonstationary P3 models.

Table 6
Returns levels in different periods, obtained by the M_{000}, and M_{001} models (Unit: 10^8 m^3).

Models	Periods				
	1960–1970	1971–1980	1981–1990	1991–2000	2001–2011
M_{000}	28.489	28.489	28.489	28.489	28.489
M_{001}	30.060	27.485	25.883	24.820	24.090

should be expressed as a very complex function of time, but we can also use other covariates by carefully investigating the driving forces of such a significant variation.

The proposed method was verified according to the Monte Carlo simulations, in which the RMSE value was computed for different quantiles of non-exceedance probabilities to compare the performance of both models. Also, these models were applied in annual runoff series and annual maximum daily precipitation series, in which significant increasing and decreasing trends could be detected. The AIC and BIC criterions were selected to compare the performance of those models. Both the simulation and case studies indicated that the nonstationary P3 model could better explain the variation in data series rather than the nonstationary GEV model.

The Monte Carlo simulations illustrated that the location parameter is most likely to be time dependent in a nonstationary P3 model. For the annual runoff, the parameter estimators obtained from the M_{001} model were less biased, but there is by no means to only consider the trends in the location parameter for the nonstationary P3 model in other regions. Although the nonstationary P3 model with a time-varying location parameter could provide the best results in most simulation cases, our analyses show that the most interesting parameter can also be the scale parameter.

In this paper, we only considered the case that the parameters of both models were dependent on time. Previous studies already indicated the climate change and human activity could significantly affect the hydrological process. Further studies can extend the use of the nonstationary P3 model in two aspects: (1) the parameters are considered to be dependent with other covariates; (2) to improve the parameter estimation methods for the nonstationary P3 model.

Acknowledgement

This study was supported by the National Key R&D Program of China (2018YFC0406501), the National Natural Science Foundation of China (Nos. 51679252 and 51409246). The meteorological data used in this study are available at http://cdc.cma.gov.cn/cdc_en/home.dd, which are provided by the National Meteorological Information Center of China Meteorological Administration. The hydrological data are obtained from the Bureau of Miyun Reservoir Management and the Haihe River Water Conservancy Commission.

Appendix A. Supplementary material

Supplementary data to this article can be found online at https://doi.org/10.1016/j.jhydrol.2018.10.035.

References

Adlouni, S.E., Ouarda, T.B.M.J., Zhang, X., Roy, B., Bobée, B., 2007. Generalized maximum likelihood estimators for the nonstationary generalized extreme value model. Water Resour. Res. 43, W03410. https://doi.org/10.1029/2005WR004545.

Benson, M.A., 1968. Uniform flood frequency estimating methods for federal agencies. Water Resour. Res. 4, 891–908.

Bobée, B., 1973. Sample error of t-year events computed by fitting Pearson type3 distribution. Water Resour. Res. 9 (5), 1264–1270.

Buckett, J., Oliver, F.R., 1977. Fitting the Pearson type 3 distribution in practice. Water Resour. Res. 13 (5), 851–852.

Cannon, A.J., 2010. A flexible nonlinear modelling framework for nonstationary generalized extreme value analysis in hydroclimatology. Hydrol. Process. 24, 673–685. https://doi.org/10.1002/hyp.7506.

Cohen Jr., A.C., 1950. Estimating parameters of Pearson type III populations from truncated samples. J. Am. Stat. Assoc. 45 (251), 411–423.

Coles, S., 2001. An Introduction to Statistical Modeling of Extreme Values. Springer, London, pp. 107.

Coles, S.G., Dixon, M.J., 1999. Likelihood-based inference for extreme value models. Extremes 2 (1), 5–23.

De, T.S., Laghari, A.N., Rauch, W., 2009. Are extreme rainfall intensities more frequent? Analysis of trends in rainfall patterns relevant to urban drainage systems. Water Sci. Technol.: J. Int. Assoc. Water Pollut. Res. 59 (9), 1769–1776. https://doi.org/10.2166/wst.2009.182.

Ding, J., Song, D.D., Yang, R.F., 1989. Further research on application of probability weighted moments in estimating parameters of the Pearson Type Three distribution. J. Hydrol. 110, 239–257.

Dodangeh, E., Soltani, S., Sarhadi, A., Shiau, J.T., 2014. Application of L-moments and Bayesian inference for low-flow regionalization in Sefidroud basin, Iran. Hydrol. Process. 28, 1663–1676. https://doi.org/10.1002/hyp.9711.

Durrans, S.R., 1992. Parameter estimation for the Pearson type 3 distribution using order statistics. J. Hydrol. 133, 215–232.

Harter, H.L., 1969. A new table of percentage points of the Pearson type III distribution. Technometrics 11 (1), 177–187.

He, Y.H., Lin, K.R., Tang, G.P., Chen, X.H., Guo, S.L., Gui, F.L., 2017. Quantifying the changing properties of climate extremes in Guangdong Province using individual and integrated climate indices. Int. J. Climatol. 37, 781–792. https://doi.org/10.1002/joc.4739.

Hosking, J.R.M., Wallis, J.R., Wood, E.F., 1985. Estimation of the generalized extreme-value distribution by the method of probability-weighted moments. Technometrics 27, 251–261.

Hosking, J.R.M., Wallis, J.R., 1993. Some statistical useful in regional frequency analysis. Water Resour. Res. 29 (2), 271–281.

IPCC, 2014. Climate change 2014: synthesis report. In: Pachauri, R.K., Meyer, L.A. (Eds.), Contribution of Working Groups I, II and III to the Fifth Assessment Report of the Intergovernmental Panel on Climate Change. IPCC, Geneva, Switzerland.
Jenkinson, A.F., 1956. The frequency distribution of the annual maximum (or minimum) values of meteorological elements. Q. J. R. Meteorol. Soc. 81, 158–171.
Kjeldsen, T.R., Jones, D.A., 2006. Prediction uncertainty in a median-based index flood method using L moments. Water Resour. Res. 42, W07414. https://doi.org/10.1029/2005WR004069.
Koutrouvelis, I.A., Canavos, G.C., 1999. Estimation in the Pearson type 3 distribution. Water Resour. Res. 35 (9), 2693–2704.
Li, J., Tan, S., 2015. Nonstationary flood frequency analysis for annual flood peak series, adopting climate indices and check dam index as covariates. Water Resour. Manage. 29, 5533–5550. https://doi.org/10.1007/s11269-015-1133-5.
Lima, C.H.R., Lall, U., Troy, T.J., Devineni, N., 2015. A climate informed model for nonstationary flood risk prediction: application to Negro River at Manaus, Amazonia. J. Hydrol. 522, 594–602. https://doi.org/10.1016/j.jhydrol.2015.01.009.
Lin, K.R., Lv, F.S., Chen, L., Singh, V.P., Zhang, Q., Chen, X.H., 2014. Xinanjiang model combined with Curve Number to simulate the effect of land use change on environmental flow. J. Hydrol. 2014 (519), 3142–3152. https://doi.org/10.1016/j.jhydrol.2014.10.049.
Lin, K.R., Lin, Y.Q., Xu, Y.M., Chen, X.H., Chen, L., Singh, V.P., 2017. Inter- and intra-annual environmental flow alteration and its implication in the Pearl River Delta, South China. J. Hydro-environ. Res. 15, 27–40. https://doi.org/10.1016/j.jher.2017.01.002.
Liu, D., Guo, S., Lian, Y., Xiong, L., Chen, X., 2014. Climate-informed low-flow frequency analysis using nonstationary modelling. Hydrol. Process. 29, 2112–2124. https://doi.org/10.1002/hyp.10360.
López, J., Francés, F., 2013. Non-stationary flood frequency analysis in continental Spanish rivers, using climate and reservoir indices as external covariates. Hydrol. Earth Syst. Sci. Discuss. 10, 3103–3142. https://doi.org/10.5194/hessd-10-3103-2013.
Martins, E.S., Stedinger, J.R., 2000. Generalized maximum-likelihood generalized extreme-value quantile estimators for hydrologic data. Water Resour. Res. 36 (3), 737–744.
Matalas, N.C., Wallis, J.R., 1973. Eureka! It fits a Pearson type 3 distribution. Water Resour. Res. 9 (2), 281–289.
Milly, P.C.D., Betancourt, J., Falkenmark, M., Hirsch, R.M., Kundzewicz, Z.W., Lettenmaier, D.P., Stouffer, R.J., 2008. Stationarity is dead: whither water management? Science 319, 573–574.
Morrison, J.E., Smith, J.A., 2002. Stochastic modeling of flood peaks using the generalized extreme value distribution. Water Resour. Res. 38 (12), 1305. https://doi.org/10.1029/2001WR000502.
Nozdryn-Plotnicki, M.J., Watt, W.E., 1979. Assessment of fitting techniques for the log Pearson type 3 distribution using Monte Carlo simulation. Water Resour. Res. 15 (3), 714–718.
Obeysekera, J., Salas, J.D., 2014. Quantifying the uncertainty of design floods under nonstationary conditions. J. Hydrol. Eng. 19, 1438–1446. https://doi.org/10.1061/(ASCE)HE.1943-5584.0000931.
Panagoulia, D., Economou, P., Caroni, C., 2014. Stationary and nonstationary generalized extreme value modelling of extreme precipitation over a mountainous area under climate change. Environmetrics 25, 29–43. https://doi.org/10.1002/env.2252.
Ribeiro-Correa, J., Rousselle, J., 1993. A hierarchical and empirical Bayes approach for the regional Pearson type III distribution. Water Resour. Res. 29 (2), 435–444.
Saf, B., 2009. Regional flood frequency analysis using l-moments for the West Mediterranean Region of Turkey. Water Resour. Manage. 23, 531–551. https://doi.org/10.1007/s11269-008-9287-z.
San, J.F., Portela, M.M., Pulido-Calvo, I., 2011. Regional frequency analysis of droughts in Portugal. Water Resour. Manage. 25, 3537–3558. https://doi.org/10.1007/s11269-011-9869-z.
Seibert, S.P., Skublics, D., Ehret, U., 2014. The potential of coordinated reservoir operation for flood mitigation in large basins – a case study on the Bavarian Danube using coupled hydrological–hydrodynamic models. J. Hydrol. 517, 1128–1144. https://doi.org/10.1016/j.jhydrol.2014.06.048.
Serinaldi, F., Kilsby, C.G., 2015. Stationarity is undead: Uncertainty dominates the distribution of extremes. Adv. Water Resour. 77, 17–36. https://doi.org/10.1016/j.advwatres.2014.12.013.
Singh, V.P., Singh, K., 1985. Derivation of the Pearson type (PT) III distribution by using the principle of maximum entropy (POME). J. Hydrol. 80, 197–214.
Song, D.D., Ding, J., 1988. The application of probability weighted moments in estimating the parameters of the Pearson Type Three distribution. J Hydrol. 101, 47–61.
Stasinopoulos, M., Rigby, B., Akantziliotou, C., 2008. Instructions on How to Use the GAMLSS Package in R, second ed.
Villarini, G., Smith, J.A., Serinaldi, F., Bales, J., Bates, P.D., Krajewski, W.F., 2009. Flood frequency analysis for nonstationary annual peak records in an urban drainage basin. Adv. Water Resour. 32, 1255–1266.
Vogel, R.W., McMartin, D.E., 1991. Probability plot goodness-of-fit and skewness estimation procedures for the Pearson type 3 distribution. Water Resour. Res. 27 (12), 3149–3158.
Yang, T., Shao, Q., Hao, Z.C., Chen, X., Zhang, Z., Xu, C.Y., Sun, L., 2010. Regional frequency analysis and spatio-temporal pattern characterization of rainfall extremes in the Pearl River Basin, China. J. Hydrol. 380, 386–405. https://doi.org/10.1016/j.jhydrol.2009.11.013.
Yu, K.X., Xiong, L.H., Gottschalk, L., 2014. Derivation of low flow distribution functions using copulas. J. Hydrol. 508, 273–288. https://doi.org/10.1016/j.jhydrol.2013.09.057.
Zhan, D.J., Ye, S.Z., 1987. Engineering Hydrology. China Water & Power Press, Beijing, China (in Chinese).
Zhang, Q., Singh, V.P., Li, J.F., 2013. Eco-hydrological requirements in arid and semiarid regions: case study of the Yellow River in China. J. Hydrol. Eng. 18, 689–697. https://doi.org/10.1061/(ASCE)HE.1943-5584.0000653.
Zucco, G., Tayfur, G., Moramarco, T., 2015. Reverse flood routing in natural channels using genetic algorithm. Water Resour. Manage. 29, 4241–4267. https://doi.org/10.1007/s11269-015-1058-z.